

# Evaluating chiral symmetry restoration through the use of sum rules

Paul M. Hohler<sup>a</sup> and Ralf Rapp<sup>b</sup>

Cyclotron Institute and Department of Physics and Astronomy, Texas A&M University, College Station, TX 77843-3366, USA

**Abstract.** We pursue the idea of assessing chiral restoration via in-medium modifications of hadronic spectral functions of chiral partners. The usefulness of sum rules in this endeavor is illustrated, focusing on the vector/axial-vector channel. We first present an update on constructing quantitative results for pertinent vacuum spectral functions. These spectral functions serve as a basis upon which the in-medium spectral functions can be constructed. A striking feature of our analysis of the vacuum spectral functions is the need to include excited resonances, dictated by satisfying the Weinberg-type sum rules. This includes excited states in both the vector and axial-vector channels. Preliminary results for the finite temperature vector spectral function are presented. Based on a  $\rho$  spectral function tested in dilepton data which develops a shoulder at low energies, we find that the  $\rho'$  peak flattens off. The flattening may be a sign of chiral restoration, though a study of the finite temperature axial-vector spectral function remains to be carried out.

## 1 Introduction

It is a long-standing problem in nuclear physics to observe chiral symmetry restoration in QCD matter. Lattice QCD computations of order parameters of the chiral transition, most notably the quark condensate, find the latter to vanish at high temperature indicative of chiral restoration [1,2]. Unfortunately, the quark condensate cannot be directly measured in experiment. Therefore, one must rely on other more indirect methods to observe chiral symmetry restoration.

A characteristic property of hadronic resonances are their spectral functions. In vacuum, resonances give rise to peak-like structures which are usually well described by a Breit-Wigner form. In medium, the hadronic states interact with the heat-bath particles inducing substantial changes of the peak-like structures in the spectral functions [3]. Since chiral restoration is a consequence of interactions with the medium, by studying the medium modifications of the spectral functions, one hopes to deduce signatures of chiral restoration. Yet, this raises several questions, for example: What type of medium modifications are expected from chiral symmetry restoration? Do different hadronic channels share generic features when approaching chiral restoration, or must we look at a large number of different resonances to glean chiral restoration? Sum rules provide some of the answers to these questions.

Sum rules, in general, relate the spectral functions via a dispersion relation to low-energy condensates, including the quark condensate among others. The spectral medium modifications expected at finite temperature are then encoded in the sum rules by changes in the condensates. Therefore, if one knows the in-medium spectral functions, from either experiment or theory, one can make predictions on the properties of the condensates, or visa versa. We will focus on two classes of sum rules here, QCD sum rules and Weinberg-type sum rules.

---

<sup>a</sup> e-mail: pmhohler@comp.tamu.edu

<sup>b</sup> e-mail: rapp@comp.tamu.edu

QCD sum rules were first introduced in Refs. [4,5] by relating the spectral function in a particular hadronic channel to an operator product expansion (OPE) containing all operators relevant for that channel (usually truncated in a series of inverse momentum transfer). The QCD sum rule is the most general relation of a spectral function to the OPE for a single hadronic channel, including both chirally symmetric and chirally breaking operators. Therefore, the medium modifications of the spectral function are driven by both types of operators. This introduces the problem that if one observes medium modifications of the spectral function, one cannot attribute these solely to chiral restoration. Thus, chiral restoration cannot be deduced by examining medium modifications of a spectral function in a single channel. However, if one considers hadronic states which are chiral partners, then the effects of the chirally symmetric operators can be canceled out so that only the chirally breaking operators survive. Therefore, to study and observe chiral symmetry restoration one is compelled to study the medium modifications of chiral partners.

The appropriate set of sum rules to study chiral partners are Weinberg-type sum rules. They refer to a set of sum rules which relate the difference of spectral function of two chiral partners to chirally breaking operators. They were developed by Weinberg [6] using current algebra relating the isovector vector and axial-vector channels. Subsequently, other sum rules of similar form have been considered [7,8], including extensions to chiral partners other than vector and axial-vector light mesons [9]. The Weinberg-type sum rules have also been extended into the medium [8]. Thereby, the medium modification of the spectral functions of the chiral partners can be related to chiral-breaking operators.

The pair of chiral partners that has been studied the most are the isovector vector and axial-vector light mesons, *i.e.*, the  $\rho$ - and  $a_1$ -meson channels. The spectral functions for both channels have been accurately measured below  $s = 3\text{GeV}^2$  by ALEPH [10] and OPAL [11] via  $\tau$  decays into an even and odd number of pions. Dilepton data from heavy-ion collisions provide information about the in-medium  $\rho$  spectral function [12,13], while the in-medium axial-vector spectral function has not been experimentally studied. Until that time, we are left to construct models of the axial-vector spectral function to study its medium modifications. Sum rules can provide an important guide in these constructions. In such a set-up, rather than inferring the condensates from the spectral functions, one can use the temperature dependence of the condensates, as computed, *e.g.*, in thermal lattice QCD, as an input to determine the spectral functions. In order to accurately constrain the features of the spectral function which are similar and those which are dissimilar between the vector and axial-vector channels, both QCD and Weinberg-type sum rules should be considered.

Several aspects of the idea of using sum rules and the known behavior of condensates in medium to ascertain properties of the in-medium spectral functions has thus far been addressed (see, *e.g.*, Part II, Sec. 2 of Ref. [3] for a review), both at finite density or at finite temperature; we here focus on the latter. Among the differences between the previous studies are the ansätze adopted for the spectral functions. While the high-energy part of the spectral functions has been routinely implemented by a continuum with a sharp threshold onset, the modeling of the low-energy resonance part has significantly evolved. Early works used a delta function to represent the ground-state resonance, while later on more realistic spectral Breit-Wigner spectral functions have been employed. In the medium, most of the previous works used QCD sum rules while few evaluated the Weinberg-type sum rules. Despite the wide range of ansätze, a few general trends have been established. The strength of the ground-state resonance, either the  $\rho$  or  $a_1$ , tends to lower energies, either through a decreasing peak position or increasing peak width (when included), or both. Furthermore, the energy associated with the threshold of the continuum also tends to shift to lower energies. In some studies, these trends were more pronounced than in others.

We intend to examine chiral symmetry restoration by ultimately studying medium modifications of spectral functions for the vector and axial-vector channels using experimental data (when available) combined with the QCD and Weinberg-type sum rules. The starting point must be a realistic description in the vacuum, where spectral functions can be quantitatively constrained using the  $\tau$ -decay data from ALEPH and further tested by Weinberg-type sum rules. The constructed spectral functions can then be used along with the QCD sum rules to determine viable vacuum values of the condensates. These results were presented in Ref. [14] and will be summarized below. These vacuum spectral functions serve as a basis for studying medium modifications at finite temperature. This investigation first addresses the construction of finite-temperature spectral functions in the vector channel using the QCD

sum rules as a constraint. Future work will be devoted to the construction of the axial-vector spectral function at finite temperature such that they satisfy both the QCD and the Weinberg-type sum rules.

This paper is organized as follows. Section 2 summarizes sum rules in vacuum and at finite temperature. In particular, it illustrates their role in studying chiral symmetry restoration. This is followed by Sec. 3 which describes the results for the constructed spectral functions in vacuum and for the vector channel at finite temperature. Conclusions are given in Sec. 4.

## 2 Sum Rules

### 2.1 Vacuum

Let us consider the current-current correlator in the vector channel, defined as

$$\Pi_V^{\mu\nu}(q) = -i \int d^4x e^{iqx} \langle T j_V^\mu(x) j_V^\nu(0) \rangle. \quad (1)$$

In vacuum, the correlator can be expressed in terms of a single function, the polarization function,  $\Pi(q^2)$ . The QCD sum rule amounts to the statement that this polarization function can be calculated in two different ways: either by a dispersion relation, or through an operator product expansion (OPE) for large values of  $Q^2 = -q^2 > 0$ . After a so-called Borel transform it reads

$$\frac{1}{M^2} \int_0^\infty ds \frac{\rho_V(s)}{s} e^{-s/M^2} = \frac{1}{8\pi^2} \left( 1 + \frac{\alpha_s}{\pi} \right) + \frac{m_q \langle \bar{q}q \rangle}{M^4} + \frac{1}{24M^4} \langle \frac{\alpha_s}{\pi} G_{\mu\nu}^2 \rangle - \frac{56\pi\alpha_s}{81M^6} \langle O_4^V \rangle \dots, \quad (2)$$

where  $\langle \bar{q}q \rangle$  is the quark condensate,  $\langle \frac{\alpha_s}{\pi} G_{\mu\nu}^2 \rangle$  the gluon condensate,  $\langle O_4^V \rangle$  the vector 4-quark condensate (explicitly given, *e.g.*, by Eq. (2.19) in Ref. [15]) and  $\rho_V \equiv -\text{Im}\Pi_V/\pi$  the vector spectral function. Typically one assumes that the 4-quark condensate can be factorized such that  $\langle O_4^V \rangle = \kappa_V \langle \bar{q}q \rangle^2$ , where  $\kappa_V$  is a parameter accounting for deviations from ‘‘factorization’’. A similar expression can be derived for the axial-vector channel [4,5]

$$\frac{1}{M^2} \int_0^\infty ds \frac{\bar{\rho}_A(s)}{s} e^{-s/M^2} = \frac{1}{8\pi^2} \left( 1 + \frac{\alpha_s}{\pi} \right) + \frac{m_q \langle \bar{q}q \rangle}{M^4} + \frac{1}{24M^4} \langle \frac{\alpha_s}{\pi} G_{\mu\nu}^2 \rangle + \frac{88\pi\alpha_s}{81M^6} \langle O_4^A \rangle \dots, \quad (3)$$

where  $\bar{\rho}_A$  is the axial-vector spectral function including the pion pole. As in the vector channel, the axial-vector spectral function is related to the quark and gluon condensates, but a different 4-quark condensate (see, *e.g.*, Eq. (2.20) in Ref. [15] for its explicit form). One may also factorize this operator as  $\langle O_4^A \rangle = \kappa_A \langle \bar{q}q \rangle^2$ . In principle,  $\kappa_V$  and  $\kappa_A$  are numerically distinct parameters, however, for the results presented here, we have assumed that they take on the same value. Note that the difference between the OPE for  $\rho_V$  and  $\bar{\rho}_A$  in vacuum is entirely given by the 4-quark condensate term. As mentioned above, the spectral functions are related to both chirally symmetric and chirally breaking operators. Therefore one can not deduce chiral restoration from either one channel separately.

Let us consider the difference between the vector and axial-vector QCD sum rules. On the left-hand-side (LHS), one simply has the difference of the two spectral functions, while on the right-hand-side (RHS) everything except the 4-quark condensates cancels. The difference in the spectral functions should be well-enough behaved so that the Borel exponential can be Taylor expanded. By equating the coefficients of same powers of  $1/M^2$  on each side, a new set of sum rules can be constructed, namely

$$\text{(WSR 1)} \quad \int_0^\infty ds \frac{\Delta\rho(s)}{s} = f_\pi^2, \quad (4)$$

$$\text{(WSR 2)} \quad \int_0^\infty ds \Delta\rho(s) = f_\pi^2 m_\pi^2 = -2m_q \langle \bar{q}q \rangle, \quad (5)$$

$$\text{(WSR 3)} \quad \int_0^\infty ds s \Delta\rho(s) = -2\pi\alpha_s \langle O_4 \rangle, \quad (6)$$

where  $\Delta\rho \equiv \rho_V - \rho_A$ . The contribution from the pion pole has been moved the RHS, and a new chirally breaking 4-quark condensate has been introduced,

$$\langle O_4 \rangle = \frac{16}{9} \left( \frac{7}{18} \langle O_4^V \rangle + \frac{11}{18} \langle O_4^A \rangle \right). \quad (7)$$

Factorization can also be applied to this 4-quark condensate,  $\langle O_4 \rangle = 16/9\kappa \langle \bar{q}q \rangle^2$  with  $\kappa = 7/18\kappa_V + 11/18\kappa_A$ . The first two equations are the Weinberg sum rules [6], with a finite quark-mass correction in the second equation [16,17,18,19], while the third equation is derived in [8]. Furthermore, a sum rule derived in [7] is associated with Weinberg-type sum rules though it is not directly derived from the QCD sum rules as the others. It reads

$$\text{(WSR 0)} \quad \int_0^\infty ds \frac{\Delta\rho(s)}{s^2} = \frac{1}{3} f_\pi^2 \langle r_\pi^2 \rangle - F_A, \quad (8)$$

where  $\langle r_\pi^2 \rangle$  is the mean squared radius of the charged pion and  $F_A$  the coupling constant for the radiative pion decay.

This simple derivation illustrates the importance of considering chiral partners. The OPE of the QCD sum rule is replaced by only chirally breaking operators. An ‘‘arbitrary’’ collection of hadronic-resonance QCD sum rules would not have resulted in such simplifications. The Weinberg-type sum rule also show that by knowing the vector and axial-vector spectral functions, one can infer the quark condensate along with additional chiral order parameters.

## 2.2 Finite Temperature

The finite-temperature extensions of both QCD and the Weinberg-type sum rules have been considered in [20] and [8], respectively. We will summarize and highlight some key points. At finite temperature, Lorentz symmetry is broken and the polarization function develops two components, usually characterized by  $\Pi_T$  and  $\Pi_L$  for the 3D transverse and longitudinal polarizations. Here we will focus on the case of vanishing 3-momentum,  $\mathbf{q} = 0$ , in which  $\Pi_L = \Pi_T$  and we can drop the labels.

At finite temperature, the condensate-values change which the sum rules translate into medium modifications of the spectral functions. Obviously, the Weinberg-type sum rules are sensitive to only chiral breaking operators, while the QCD sum rules are sensitive to both chirally breaking and chirally symmetric. The QCD sum rules are particularly useful when the focus is on a single channel, not the relation between different channels.

It turns out that the construction of the finite-temperature Weinberg sum rules simply amounts to replacing the vacuum spectral functions and operators with their values at finite temperature in the expressions above [8]. The pion pole in general develops a non-trivial spectral distribution and so its contribution is included back into the axial-vector spectral function. One has

$$\text{(WSRFT 1)} \quad \int_0^\infty ds \frac{\Delta\bar{\rho}(s)}{s} = 0, \quad (9)$$

$$\text{(WSRFT 2)} \quad \int_0^\infty ds \Delta\bar{\rho}(s) = 0, \quad (10)$$

$$\text{(WSRFT 3)} \quad \int_0^\infty ds s \Delta\bar{\rho}(s) = -2\pi\alpha_s \langle O_4 \rangle_T, \quad (11)$$

where  $\Delta\bar{\rho}(s) = \rho_V(s) - \bar{\rho}_A(s)$ . A derivation from the finite temperature QCD sum rules is also possible. These equations show that at chiral restoration where the pion pole and the 4-quark condensate vanish, the vector and axial-vector spectral functions should be degenerate.

For the QCD sum rules, the vacuum spectral function is replaced by the finite temperature spectral function, while the OPE becomes more involved. In addition to the scalar condensates, which figure in vacuum and develop a temperature dependence, new non-scalar condensates appear. The latter are

possible because of the breaking of Lorentz symmetry in medium. They are classified by their dimension, spin, and twist, where twist = dimension - spin (scalar operators have twist-0). The resulting sum rule reads

$$\frac{1}{M^2} \int_0^\infty ds \frac{\rho_V^T(s)}{s} e^{-s/M^2} = \frac{1}{8\pi^2} \left(1 + \frac{\alpha_s}{\pi}\right) + \frac{m_q \langle \bar{q}q \rangle_T}{M^4} + \frac{1}{24M^4} \langle \frac{\alpha_s}{\pi} G_{\mu\nu}^2 \rangle_T - \frac{56\pi\alpha_s}{81M^6} \langle O_4^V \rangle_T + \frac{\langle O^{d=4,\tau=2} \rangle_T}{M^4} + \frac{\langle O^{d=6,\tau=2} \rangle_T}{M^6} + \frac{\langle O^{d=6,\tau=4} \rangle_T}{M^6}, \quad (12)$$

where  $\langle O^{d=4,\tau=2} \rangle_T$ ,  $\langle O^{d=6,\tau=2} \rangle_T$ , and  $\langle O^{d=6,\tau=4} \rangle_T$  represent the twist-2 and twist-4 operators. A discussion of the higher-twist operators can be found in [20,21,22]. A similar expression can be derived for the axial-vector channel. Note that all of the higher-twist operators are chirally symmetric and so are identical between the two channels.

To determine the modifications of the condensates at low temperatures, one may invoke the dilute gas approximation which amounts to a generic expression of type

$$\langle O \rangle_T \simeq \langle O \rangle_0 + d_X \int \frac{d^3k}{(2\pi)^2 2E_k} \langle X(\mathbf{k}) | O | X(\mathbf{k}) \rangle, \quad (13)$$

where  $\langle O \rangle_0$  is the vacuum value of a given operator  $\langle X(\mathbf{k}) | O | X(\mathbf{k}) \rangle$  is the matrix element of the same operator within hadron  $X$ , and  $d_X$  is the degeneracy factor for that hadron. For the vacuum values of the operators we follow Ref. [14], namely  $\langle \bar{q}q \rangle = (-0.25 \text{ GeV})^3$ ,  $\langle \frac{\alpha_s}{\pi} G_{\mu\nu}^2 \rangle = 0.022 \text{ GeV}^4$ ,  $\langle O_4^V \rangle = \kappa \langle \bar{q}q \rangle^2$  with  $\kappa = 2.1$ . The expansion (13) also holds for the higher-twist operators with a vanishing vacuum value. This reduces the problem to determining the matrix elements  $\langle X(\mathbf{k}) | O | X(\mathbf{k}) \rangle$ . To do so, we assume that the medium can be described by a hadron resonance gas (HRG) along the lines of [23]. All reliably known hadrons with a mass less than 2 GeV [24] have been considered. The temperature dependence for the quark and 4-quark condensates is augmented around the transition temperature beyond the consideration of the HRG such that the quark condensate better fits lattice calculations and that the 4-quark condensates vanish at the same temperature as the quark condensate. The results are depicted in Fig. 1. Further details concerning the HRG estimate of the higher-twist operators will be presented in future work. The temperature dependence of the condensates increases the OPE side relative to the vacuum. Via the QCD sum rule, this increase is manifest in the spectral function through an increased spectral strength at lower energies. This will be apparent when we discuss the results for the finite-temperature vector spectral function below.

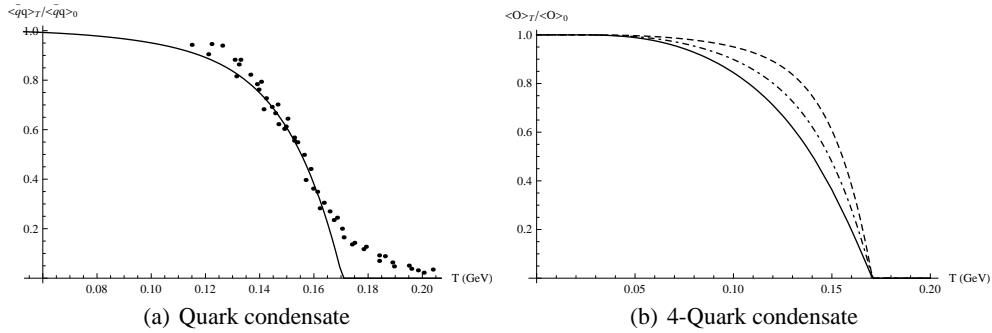


**Fig. 1.** a) Temperature dependence of quark condensate relative to its vacuum value compared with lattice data points [1]. b) Temperature dependence of vector (solid curve) and axial-vector (dot-dashed curve) 4-quark condensates relative to their vacuum values compared with the temperature dependence of the quark condensate relative to its vacuum value (dashed curve).

### 3 Spectral Functions and Numerical Evaluation

Having described the relevant sum rules in vacuum and shown how they are modified at finite temperature, we are now in position to construct model spectral functions, including experimentally determined properties, and test whether their medium modifications satisfy the sum rules. We shall begin in the vacuum and construct spectral functions for both the vector and axial-vector channels. The results presented here are a summary of those found in [14].

For both channels, the spectral function is constructed from three parts,

$$\rho_V(q_0) = \rho_V^{\text{gs}}(q_0) + \rho_V^{\text{ex}}(q_0) + \rho^{\text{cont}}(q_0) \quad (14)$$

where  $\rho_V^{\text{gs}}$ ,  $\rho_V^{\text{ex}}$  and  $\rho_V^{\text{cont}}$  correspond to the ground-state resonance, an excited-state resonance and a perturbative QCD (pQCD) continuum, respectively. There are three critical features about this ansatz. First, for the  $\rho(770)$  contribution to the spectral function, we employ the microscopic model of [25], which satisfies the low-energy  $\tau$ -decay data well [26]. It has the added advantage that its medium modifications have been computed and successfully applied to experiment [27,28]. This provides a strong basis for forthcoming investigations in medium. Second, the continuum contribution for the vector and the axial-vector channels is postulated to be identical. This is to be expected at higher energies where pQCD can be used to calculate its contribution. We have extended this premise to all energies, and chosen a continuous onset with energy, *i.e.* a discontinuous threshold is not considered. Third, the first excited states are postulated (which, in fact, emerges as a consequence of the degenerate continuum). The pertinent spectral functions for the  $\rho'$  and  $a'_1$  are parameterized Breit-Wigner functions (as is the  $a_1$ , as a placeholder for a forthcoming microscopic model).

The parameters of the model were chosen such that the resulting spectral functions satisfactorily agree with the  $\tau$ -decay data and that Weinberg-type sum rules 0 – 2 are satisfied. The comparison of the spectral functions with data is illustrated in Fig. 2. We find that by postulating identical pQCD the continua between the two channels, one is forced to consider their onset occurring at higher energies as compared with previous studies. This is due to the relatively large valley in the axial-vector spectral function around  $2.2 \text{ GeV}^2$ . The larger continuum onset, in turn, requires the inclusion of the  $\rho'$  so that the vector spectral function agrees with the  $\tau$ -decay data, which can be achieved with contributions from only the  $\rho$ ,  $\rho'$  and  $a_1$  (plus continua). However, with this input the Weinberg-type sum rules are violated, in a way that the LHS largely exceeds the RHS, the more so the higher the moment. This clearly points to a missing “high”-energy strength in the axial-vector spectral function. We are therefore led to postulate the presence of an excited axial-vector meson, namely the  $a'_1$ . There is large uncertainty in the  $\tau$ -decay data at higher energies, sufficient enough to fit an excited state within the error bars (and/or beyond the data range), as shown in Fig. 2(b). We deduce a mass of the excited state of around  $1.8 \text{ GeV}$  and a width of around  $200 \text{ MeV}$ . In Table 1, we collect the resulting values for the Weinberg-type sum rules (a positive sign means that the vector channels contribution is greater). The agreement with the three sum rules is much improved after inclusion of the  $a'_1$ , especially for WSR-0, -1 and -2, which we used as criteria to infer the existence of the excited state.

The constructed spectral functions are subsequently used in the QCD sum rules to determine the values of the gluon condensate and the factorization parameters  $\kappa_V$  and  $\kappa_A$ . The vacuum values of these quantities are not as well established, especially the factorization parameters. We assume that the two  $\kappa$ 's are numerically the same. By minimizing the average deviation between the two sides of the QCD sum rules as described in [29,30,14], we find  $\kappa = 2.1_{-2}^{+3}$  and  $\langle \frac{\alpha_s}{\pi} G_{\mu\nu}^2 \rangle = 0.022 \pm 0.002 \text{ GeV}^4$ . The optimized average deviations for vector and axial-vector channels are 0.24% and 0.56%, respectively.

WSR	0 <sup>th</sup>	1 <sup>st</sup>	2 <sup>nd</sup>	3 <sup>rd</sup>
% agreement	-1.28%	~ 0%	~ 0%	-96%

**Table 1.** Percent disagreement between LHS and the RHS of the Weinberg-type sum rules resulting from our fit.

The vacuum spectral functions can be used as a basis for investigating medium modifications at finite temperature. For the remainder of this section, preliminary results for the finite temperature

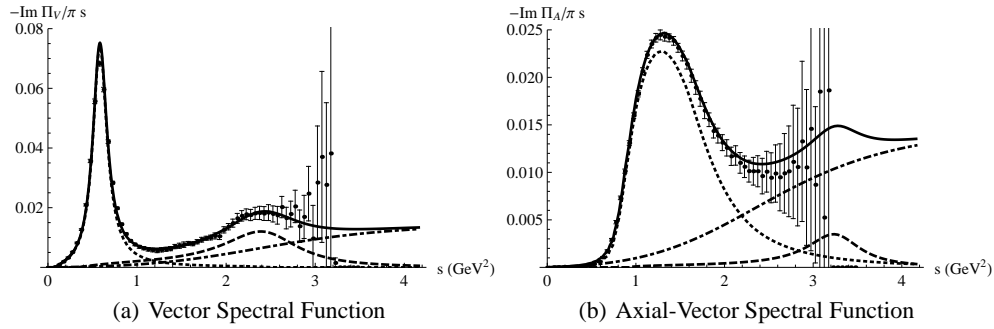


**Fig. 2.** Spectral functions for the vector and axial-vector channels compared to experimental data for hadronic  $\tau$  decays by the ALEPH collaboration [10]. The different curves highlight the contributions to the total spectral function (solid curve) from the ground-state resonance (dotted curve), the excited resonance (dashed curve), and the continuum (dot-dashed curve).

vector spectral function will be presented. The finite-temperature axial-vector spectral function will be discussed in future work.

For the finite-temperature vector spectral function, we will primarily be using the QCD sum rule to constrain it. We have argued above that the OPE side will increase with temperature. This implies that the medium modification of the spectral function will be such to increase its spectral strength. In connection with the Borel transform, this is realized by additional spectral strength at lower energies.

The ansatz for the finite-temperature spectral function is divided into the same basic three parts as the vacuum ansatz: contributions from the ground state, an excited state and from the pQCD continuum. As discussed above, for the contribution from the  $\rho$  meson, we use the spectral function of [25,27]. For the continuum, we postulate no temperature dependence. This is contrary to previous studies which deduced a decrease in the continuum. However, as we will demonstrate, we will still recover a spectral function which has the appearance of a moving continuum, even if the continuum actually has no temperature dependence. This assumption is also consistent with expectations from pQCD. For the  $\rho'$ , the medium modifications are implemented by parameterizing the Breit-Wigner spectral function with adjustable mass, width and coupling to the vector current. At each temperature, the necessary adjustments to these parameters are made so that the QCD sum rule is satisfied. As in the case of the vacuum, we use the average deviation as a measure for the agreement of the QCD sum rules. We further insist that parameters are monotonic with temperature; this ensures that un-physical parameterizations such as a width narrowing with temperature do not occur. The resulting spectral functions at select temperatures are shown in Fig. 3.

Two striking features of the finite-temperature spectral function are the development of a low-energy shoulder to, and the reduction of, the  $\rho$  peak (both pivotal to the description of dilepton data), as well as the reduction of the  $\rho'$  peak. The formation of new low-energy strength in the medium was to be expected from the QCD sum rules, however, the shoulder actually adds too much strength. Therefore the  $\rho'$  must reduce in strength (as shown) to compensate for the extra strength in the  $\rho$  peak. The reduction of the  $\rho'$  peak (along with a slight broadening) flattens the higher energy region of the spectral function. The resulting flattened spectral function starts to resemble a flat continuum with a lower threshold. Therefore the effect which has been previously associated with a moving continuum is in this model realized via the dissociation of the  $\rho'$ . That this dissociation occurs prior to that of the  $\rho$  is in line with the idea of sequential dissociation of resonances with increasing temperature (not unlike heavier quarkonia). Lastly, the flattening of the spectral function may also signal chiral restoration. The vacuum axial-vector spectral function has a majority of its strength centered at an energy around the valley of the vector spectral function. Thus, one could surmise that the filling of the "vector valley" will be accompanied by a reduction of strength in the axial-vector channel so that chiral restoration emerges, not unlike the well-known "chiral mixing" in a dilute pion gas [31]. For a HRG this largely remains a speculation until the medium modifications of the axial-vector spectral function are determined more explicitly.

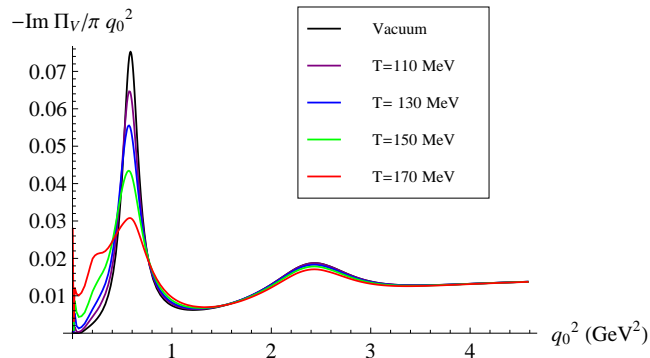


Fig. 3. (Color online) Spectral functions for the vector channel at different temperatures.

## 4 Conclusion

We have illustrated the role of sum rules in examining chiral symmetry restoration in hot matter. Results for the construction of vacuum spectral functions for the vector and axial-vector channels have been presented. Based on a quantitative analysis of existing vacuum data, we are led to postulate the existence of an excited axial-vector resonance in order to satisfy the Weinberg-type sum rules. Preliminary results from in-medium vector spectral functions have also been presented. We have constructed the latter starting from an in-medium  $\rho$  spectral function from microscopic hadronic effective field theory which is consistent with SPS dilepton data. The spectral function further includes medium modifications of the  $\rho'$  peak as constrained by finite-temperature QCD sum rules, while no medium modification to the continuum was considered. We have found the resulting spectral functions to be consistent with the idea that the medium broadens the states and reduces the strength of the resonances, *i.e.*, both  $\rho$  and  $\rho'$ . We have observed indications for a sequential dissociation, and a rearrangement of spectral strength toward the energy regions of the axial-vector resonance, suggestive of chiral restoration. However, it is important to emphasize that in order to establish chiral restoration, either experimentally or theoretically, quantitative knowledge of the spectral functions for both chiral partners are required. Therefore, the present study is only a beginning as the medium modifications of the axial-vector spectral function remain to be calculated. This work is currently underway. Ideally this would also trigger a renewed emphasis to experimentally measure the in-medium axial-vector spectral function, even in the dilute phases of nuclear collisions or in elementary production processes off ground-state nuclei.

## References

1. S. Borsanyi *et al.* [Wuppertal-Budapest Collaboration], JHEP **1009**, (2010) 073.
2. A. Bazavov *et al.*, Phys. Rev. D **85**, (2012) 054503.
3. B. Friman, (ed.), C. Hohne, (ed.), J. Knoll, (ed.), S. Leupold, (ed.), J. Randrup, (ed.), R. Rapp, (ed.) and P. Senger, (ed.), Lect. Notes Phys. **814**, (2011) 1.
4. M. A. Shifman, A. I. Vainshtein and V. I. Zakharov, Nucl. Phys. B **147**, (1979) 385.
5. M. A. Shifman, A. I. Vainshtein and V. I. Zakharov, Nucl. Phys. B **147**, (1979) 448.
6. S. Weinberg, Phys. Rev. Lett. **18**, (1967) 507.
7. T. Das, V. S. Mathur and S. Okubo, Phys. Rev. Lett. **19**, (1967) 859.
8. J. I. Kapusta and E. V. Shuryak, Phys. Rev. D **49**, (1994) 4694.
9. T. Hilger, B. Kampfer and S. Leupold, Phys. Rev. C **84** (2011) 045202.
10. R. Barate *et al.* [ALEPH Collaboration], Eur. Phys. J. C **4**, (1998) 409.
11. K. Ackerstaff *et al.* [OPAL Collaboration], Eur. Phys. J. C **7**, (1999) 571.
12. R. Arnaldi *et al.* [NA60 Collaboration], Phys. Rev. Lett. **96**, (2006) 162302.

Resonance Workshop at UT Austin

13. D. Adamova, G. Agakichiev, D. Antonczyk, H. Appelshauser, V. Belaga, J. Bielicikova, P. Braun-Munzinger and O. Busch *et al.*, Phys. Lett. B **666**, (2008) 425.
14. P. M. Hohler and R. Rapp, arXiv:1204.6309 [hep-ph].
15. S. Leupold, Phys. Rev. C **64**, (2001) 015202.
16. P. Pascual and E. de Rafael, Z. Phys. C **12**, (1982) 127.
17. S. Narison, Z. Phys. C **14**, (1982) 263.
18. R. D. Peccei and J. Sola, Nucl. Phys. B **281**, (1987) 1.
19. V. Dmitrasinovic, Nucl. Phys. A **686**, (2001) 379.
20. T. Hatsuda, Y. Koike and S. -H. Lee, Nucl. Phys. B **394**, (1993) 221.
21. S. Leupold and U. Mosel, Phys. Rev. C **58**, (1998) 2939.
22. S. Zschocke, O. P. Pavlenko and B. Kampfer, Eur. Phys. J. A **15**, (2002) 529.
23. S. Leupold, J. Phys. G **32**, (2006) 2199.
24. K. Nakamura *et al.* (Particle Data Group), J. Phys. G **37**, (2010) 075021.
25. M. Urban, M. Buballa, R. Rapp and J. Wambach, Nucl. Phys. A **673**, (2000) 357.
26. R. Rapp, Pramana **60**, (2003) 675.
27. R. Rapp and J. Wambach, Eur. Phys. J. A **6**, (1999) 415.
28. F. Riek, R. Rapp, T. S. Lee and Y. Oh, Phys. Lett. B **677**, (2009) 116.
29. D. B. Leinweber, Annals Phys. **254**, (1997) 328.
30. S. Leupold, W. Peters and U. Mosel, Nucl. Phys. A **628**, (1998) 311.
31. M. Dey, V. L. Eletsky and B. L. Ioffe, Phys. Lett. B **252**, (1990) 620.